Title
Geophysical Monitoring Shows that Spatial Heterogeneity in Thermohydrological Dynamics Reshapes a Transitional Permafrost System

Journal
Geophysical Research Letters, 48(6)

ISSN
0094-8276

Authors
Uhlemann, S
Dafflon, B
Peterson, J
et al.

Publication Date
2021-03-28

DOI
10.1029/2020gl091149

Peer reviewed

Geophysical Monitoring Shows that Spatial Heterogeneity in Thermohydrological Dynamics Reshapes a Transitional Permafrost System

S. Uhlemann[1], B. Dafflon[1], J. Peterson[1], C. Ulrich[1], I. Shirley[1,2], S. Michail[3], and S. S. Hubbard[1]

[1]Lawrence Berkeley National Laboratory, Earth and Environmental Sciences Area, One Cyclotron Road, CA 94720 Berkeley, USA

[2]University of California, CA 94720 Berkeley, USA

[3]ETH Zurich, Institute of Geophysics, Sonneggstrasse 5, 8092 Zurich, Switzerland

Corresponding author: Sebastian Uhlemann (suhlemann@lbl.gov)

Key Points:

- Transitional permafrost systems evolve through complex infiltration pathways and energy fluxes, including lateral flow
- Snow pack and vegetation distribution play major role in permafrost thermohydrological responses
- Monitoring shows spatially variable thermohydrological responses and intra- to inter-annual dynamics in discontinuous permafrost systems

Abstract

Climate change is causing rapid changes of Arctic ecosystems. Yet, data needed to unravel complex subsurface processes are very rare. Using geophysical and in-situ sensing, this study closes an observational gap associated with thermohydrological dynamics in discontinuous permafrost systems. It highlights the impact of vegetation and snow thickness distribution on subsurface thermohydrological properties and processes. Large snow accumulation near tall shrubs insulates the ground and allows for rapid and downward heat flow. Thinner snowpack above graminoid results in surficial freezing and prevents water from infiltrating into the subsurface. Analyzing short term disturbances, we found that lateral flow could be a driving factor in talik formation. Inter-annual measurements show that deep permafrost temperatures increased by about 0.2°C over two years. The results, which suggest that snow-vegetation-subsurface processes are tightly coupled, will be useful for improving predictions of Arctic feedback to climate change, including how subsurface thermohydrology influences CO_2 and CH_4 fluxes.

Plain Language Summary

When permafrost thaws, water can flow quicker through the ground, creating a very complex subsurface flow system. In this study, we gain detailed insight into these complex processes by measuring the electrical resistivity of the ground daily. Our results show that the type of vegetation and the snowpack that accumulates on it in winter control the temperatures of the ground, and therefore also how water flows. Above tall shrubs snow accumulates much more than above grass. Therefore, temperatures below shrubs are warmer and water and energy from snowmelt and rain can flow through the ground quickly, while colder temperatures below the grass prevent this rapid flow. Longer-term dynamics show us that the temperature of permafrost at about 10m depth increased by 0.2°C over a period of two years. The results of this study should be useful for improving predictions of Arctic feedback to climate change.

1 Introduction

The average temperature of permafrost has increased globally by about 0.4°C in the last century. This is partly due to the Arctic amplification of an increase in air temperature in the Northern Hemisphere, but also due to increased snow thickness, especially in areas of discontinuous permafrost (Biskaborn et al., 2019). This change in temperature changes the physical properties of the subsurface, with impacts on infrastructure (Hjort et al., 2018), groundwater resources, vegetation distribution (Jorgenson et al., 2013; Lloyd et al., 2003), carbon and nitrogen cycling (Petrone et al., 2006), and greenhouse gas emissions (Jansson & Taş, 2014), leading to further acceleration of climate change.

Jorgenson et al. (2010) show that complex feedbacks exist between permafrost dynamics and topography, vegetation distribution, snow pack, ground temperature, and subsurface hydrological properties. Rising permafrost temperatures cause increasing hydraulic conductivities in the soil to bedrock column, enabling or enhancing surface water-groundwater interactions, changes to the groundwater residence times, and eventual alterations to ground- and stream-water temperature and compositional dynamics (Hinzman et al., 2005; Ireson et al., 2013). These changes in hydrology enhance the importance of the deeper subsurface for carbon and nutrient cycling (Koch et al., 2013; Lyon et al., 2010), and are particularly important for discontinuous permafrost, which accounts for 19% of the Northern Hemisphere's land surface that is covered by permafrost, i.e. 4.4×10^6 km^2 (Zhang et al., 2003). This region is characterized by a complex distribution of perennial frozen and unfrozen ground, and hence areas of year-round unfrozen ground within permafrost landscapes, or taliks. Arctic discontinuous permafrost is usually "warm" (likely >-3 °C), and a mean temperature increase of 0.2 ± 0.1°C has been recorded over the last decade (Biskaborn et al., 2019). These changes are forming a transitional permafrost environment, where areas of continuously frozen ground are becoming unfrozen, impacting microbial and soil processes, hydrology, and flora and fauna (Vincent et al., 2017; Woo et al., 2008). We currently lack data and predictive understanding of how these complex interactions influence the evolution of this ecosystem - now and in the future. Gaining information on the factors controlling near-surface ground temperatures and water distribution is critical to being able to predict the fate of Arctic ecosystems and its feedback to climate (Walvoord & Kurylyk, 2016).

Measuring thermohydrological properties and processes in permafrost environments is difficult due to inaccessibility, sensitive ecosystems, and the harsh Arctic environment. Hence, data associated with surface water-groundwater interactions, and infiltration and subsurface flow processes are sparse (Bring et al., 2016). Geophysical techniques are known to complement point observations and to assess the intermediate depths (1 - 10's of m) at spatial and temporal resolutions critical to understanding the impact of climate change on permafrost hydrological dynamics (Dafflon et al., 2017; Kneisel et al., 2008; Minsley et al., 2012; Parsekian et al., 2019). Electrical properties of soils, particularly at temperatures below freezing, are highly sensitive to variations in temperature (Wu et al., 2017). Below the freezing point, resistivity changes are several orders of magnitude larger than above freezing and depend on the initial liquid water content and the pore size distribution (Ming et al., 2020). Hence, in frozen environments, monitoring changes in subsurface electrical resistivity can highlight variations in subsurface temperature and hydrological conditions (Farzamian et al., 2020; Krautblatter et al., 2010).

By combining geophysical and in-situ point sensing along a single transect, this study aims at providing insight to two questions: (1) how spatially and temporarily variable are thermohydrological properties and processes in transitional permafrost environments, and (2) what is the impact of topography, vegetation and snow-pack distribution on those properties? This integrated, spatially and temporally resolved study closes an observational gap with regards to thermohydrological fluxes and deep permafrost dynamics that currently exists in the understanding of permafrost-dominated systems. While the observations are representative for a small domain, the processes that were observed are likely valid for a wide range of Arctic permafrost environments. To our knowledge, this is the first study to remotely monitor sub-seasonal through multi-annual thermohydrological processes in transitional permafrost environments at spatiotemporal resolutions required to discover controls on subsurface infiltration and temperature dynamics that ultimately shape this evolving Arctic ecosystem.

2 Study Site and Methods

A permafrost monitoring site was established on the Seward Peninsula (64.72°N, 165.94°W) in September 2017 (Fig. 1A). The study site is located in the Southern part of the Seward peninsula, which is classified as discontinuous permafrost (Brown et al., 2002) The monitoring site includes a 127m long transect located within the lower elevations of a watershed, which is a focus of the Department of Energy Next Generation Ecosystem Experiments (NGEE)

Arctic project. The transect is perpendicular to the main slope gradient and crosses two different vegetation types; one covered with graminoid and the other primarily with tall shrubs (Léger et al., 2019). Graminoids are vascular, herbaceous plants with a morphology similar to grass that grow up to a few 10's of cm, while the tall shrubs here are mainly composed of willow with heights up to 2m. At five locations along this transect (Fig. 1A) soil temperature and moisture content are measured hourly at 0.1, 0.2, 0.3, and 0.4m depth, with additional temperature measurements at 1.5m below ground level (bgl, Fig. 1B); several soil cores were recovered along the transect for laboratory analysis (see supplementary information). Rainfall and air temperatures were recorded at a local weather station (Busey et al., 2017), while winter snow fall records were obtained from a station at Nome Airport (NOAA-ID: GHCND:USW00026617). Snow thickness was measured at 1m intervals across the transect in late March 2018 and 2019.

An Electrical Resistivity Tomography (ERT) monitoring transect, using 128 electrodes spaced at 1m, is the primary dataset for this study. ERT data were acquired daily between late March and September of 2018 and 2019 using dipole-dipole measurements. Data were filtered based on an error model (Tso et al., 2017) that was developed from reciprocal measurements acquired in September 2017 and March 2018. To transform measured transfer resistances to subsurface resistivity models, the acquired data were inverted using E4D (Johnson et al., 2010) applying a conventional L2-norm regularization, with stronger spatial than temporal constraints (ratio 2/1). The inversions converged at root-mean-squared misfits between measured and modelled data of 1.5% to 4.3%. The depth of investigation of the ERT measurements was determined using an approach introduced by Oldenburg & Li (1999), and confirmed that those measurements were sensitive to depths of ~15m bgl.

3 Data Overview

The baseline electrical resistivity model (Fig. 1B) of September 2017 shows a conductive upper layer varying in thickness, which can be related to the unfrozen organic and soil layers. It is underlain by a highly resistive layer, which is representative of permafrost. The highest resistivities (~1000Ωm) were recorded in the center of the profile at depths >5m below the graminoid area. High resistivity features were also imaged at similar depths below the eastern and western shrubs (~900 and ~800Ωm, respectively), but end of summer soil temperatures recorded at 1.5m bgl (squares above Fig. 1B) were higher in the shrub than in the graminoid area (4.6°C and -0.1°C, respectively). Similar spatial trends are observed in snow thickness distribution. The thickest snow pack was recorded in the shrub areas (1.83 ± 0.27m) and the thinnest over the graminoid (0.70 ± 0.24m). The winter periods of 2017/2018 and 2018/2019 had mean air temperatures of -8.0 ± 5.7°C and -8.9 ± 6.7°C, respectively, and summer precipitation accumulated to 226.9 and 451.3mm in 2018 and 2019, respectively. With the exception of the 2019 rainfall, these values are within the long-term average and representative of the climate of the Seward Peninsula.

Figs. 1C and D show the temporal variability in electrical resistivity for four zones (with respect to the baseline measurement), representing shallow (surface to 2m bgl, boxes 1 and 3) and deep (8 to 14m bgl, boxes 2 and 4) areas underneath the graminoid and shrub areas. From the start of monitoring in March to the onset of snowmelt, resistivities stay at their yearly maxima reflecting cold and (below the graminoid) frozen conditions. The start of snowmelt causes a rapid decrease in the shallow resistivities underneath the shrubs (27% in 10 days), and a slower decrease underneath the graminoid (5% during the same period). This is related to thawing of the near surface and infiltration of snowmelt. Deeper parts of the model show comparable trends and time lags, but smaller amplitudes. Although soil moisture at 0.1m depth shows a clear response to snowmelt and rainfall events, soil moisture at 0.4m bgl below the shrubs remains almost constant throughout the year (27.1 ± 1.7%), indicating fully saturated conditions (see supplementary information). Below the graminoid area, soil moisture changes at 0.4m bgl can be linked to the freeze and thaw cycles, and hence to changes in liquid water content. Given the saturated conditions, we can assume that the observed resistivities are mainly affected by changes in temperature conditions.

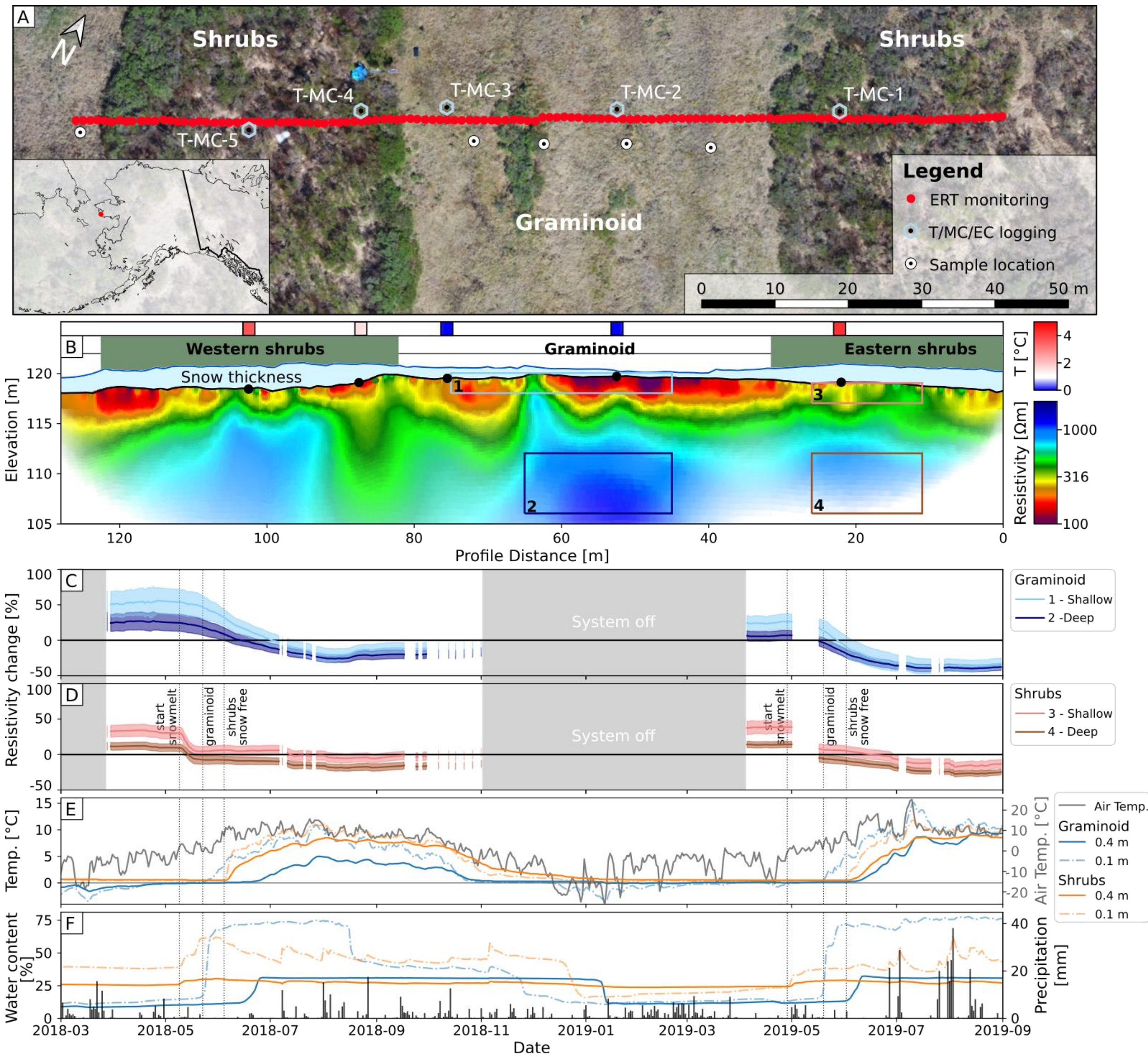

Figure 1 Sensor installation and annual variability of electrical resistivity, soil temperature, and water content. (A) Overview map of the monitoring installation. The center of the monitoring transect is characterized by graminoid, and both ends by dense tall shrubs. Inset shows the location within Alaska, US. (B) Baseline electrical resistivity model (09/2017), with low resistivities in warm and high resistivities in cold colors. Resistivities with a DOI > 0.15 (Oldenburg & Li, 1999) are blended out. Shown are sensor locations, areas for which resistivity is analyzed, soil temperatures (1.5m bgl, colored squares), and snow thickness (04/2018). (C, D)

Change in electrical resistivity with respect to baseline measurement for areas indicated in (B). (E) Temperature variation at 0.1 and 0.4m bgl, and air temperature records. (F) Moisture content at the same locations as in (C), and measured precipitation. Temperature and moisture data were measured at T-MC-1 and T-MC-2.

4 Heavy rainfall supplies energy deep into permafrost system

Rainfall can provide significant energy input into permafrost systems, causing rapid changes in soil temperature to depths >0.5m bgl and increasing methane emissions from thawing permafrost (Neumann et al., 2019). Yet, depth and laterally resolved data are sparse, particularly at depths greater than 0.5m. To explore this phenomena, we focus on a natural rainfall event that took place in August 2019, accumulating 127.1mm rainfall in four days (Fig. 2). While the shallowest soil moisture sensor in the shrubs recorded increasing water content in response to the rainfall (particularly within the eastern shrubs), sensors 0.4m bgl remained almost constant throughout August (39.0 ± 0.6%, 27.9 ± 0.5%, and 31.0 ± 0.01% for eastern and western shrubs, and graminoid, respectively).

Since soil moisture remained mostly unchanged during and past this storm event, we consider electrical resistivity changes to be associated mostly with changes in temperature. The main precipitation event occurred on August 2nd (65mm), and within one day caused a 1.0°C and 0.2°C increase in soil temperature at 0.4 m bgl in the western and eastern shrubs, respectively. The shrub areas show a general warming trend until mid-August 2019, followed by decreasing temperatures towards the end of the month (Fig. 2A). In the graminoid area, these trends appear delayed, showing increasing temperatures five days after the storm event and continuing until the end of the month. The subsurface electrical resistivities show a decreasing trend in the first three days after the rainfall event, after which resistivities remain reasonably stable until increasing towards the end of August (Fig. 2A). Amplitudes in the resistivity changes are higher in the shallow than in the deep subsurface. While this could be an effect of the reduced sensitivity of the ERT measurement with depth, this decrease in amplitude is also expected given the imaged processes.

The changes in the electrical resistivity (with respect to a measurement prior to the event) show distinct patterns for the two shrub units and the graminoid (Fig. 2D-E). Fig. 2D shows the western shrubs to be dominated by decreasing resistivities between -5 and -20%, while the eastern shrubs show small reductions in the shallow subsurface only. Lateral heat flow was observed at depths >5m bgl, where a decreasing resistivity trend advanced from the western shrubs toward the graminoid. Resistivities decreased further in the two weeks past the storm event. No significant decrease was recorded in the deeper sections below the graminoid.

We associate those rapid changes to heat advection dominating the thermodynamics, as diffusion would be a slower processes. Heat advection has been shown to accelerate permafrost degradation (Rowland et al., 2011), particularly in response to rainfall events (Mekonnen et al., 2020). Chen et al. (2020) present a field study showing temperature data that suggests a thermal response of permafrost to rainfall to depths >7m within 4 days past rainfall events. The variable magnitude in changes observed across the transect can be explained by different initial temperatures and hence ice content. Based on the imaged electrical resistivities, graminoid and eastern shrubs are expected to correspond to lower subsurface temperatures and larger ice content than the western shrubs. Given this initial situation and assuming that the resistivity change is indicative of coupled thermohydraulic flow dynamics, thermal and hydraulic conductivities are likely higher underneath the western shrubs (Hinzman et al., 1991; Thomas et al., 2009), facilitating rapid movement of precipitation energy into depths >1m. With higher ice content underneath the eastern shrubs and graminoid, hydraulic conductivities are lower and energy from the precipitation is likely not being transported vertically into the deeper subsurface, but horizontally through lateral flow.

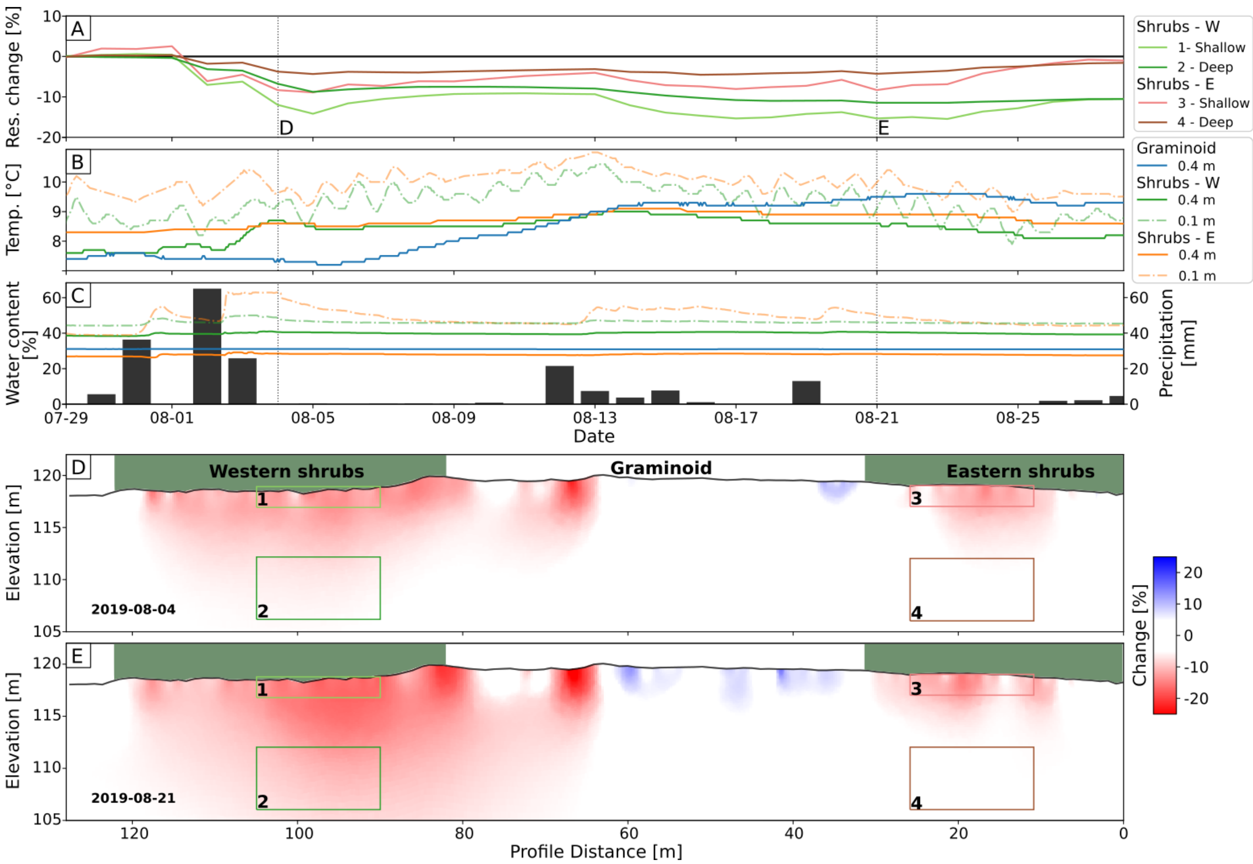

Figure 2 Heavy rainfall causes rapid change in electrical resistivity underneath the western tall shrubs. (A) Change in electrical resistivity with regards to a measurement prior to the onset of a rainfall event (07/29/2019). (B-C) recorded soil temperature and moisture content from in-situ sensors, and precipitation. (D-E) distribution of changes in electrical resistivity at two dates.

5 Snowmelt processes highlight spatially variable dynamics

Snowmelt provides another natural tracer to study the permafrost thermohydrological processes and to image the feedback to variabilities in snow thickness. Here, we focus on the effects of snowmelt in May 2018 (Fig. 3). Daily photographs of the site confirmed that the graminoid was mostly snow free on May 22nd, while the shrub dominated area, due to thicker snowpack, showed snow free conditions two weeks later, on June 5th. These dates coincide with an increase in shallow and deep temperatures (Fig. 3B). Liquid water content in the shallow subsurface below the shrubs increases beginning May 8th, which was defined as the start of snowmelt. Coinciding with this date, subsurface electrical resistivities decrease throughout the imaging domain, with a more rapid decrease below the shrubs. The graminoid area shows a slower response and continuously decreasing resistivities throughout the analyzed period. The shrub areas show increasing resistivities once they became snow free.

More detail on the subsurface thermohydrological response to snowmelt can be inferred from the imaged changes in resistivity. Initially, minimal change was recorded below the graminoid, whereas the shrub areas showed decreasing resistivity >5m bgl two weeks after the start of snowmelt (Fig. 3D). This difference can be explained by the surface temperature conditions in response to the snow thickness distribution. While below the thick snowpack of the shrubs (1.83 ± 0.27m) surface temperatures remained above 0°C throughout the winter, the thinner snowpack (0.70 ± 0.24m) of the graminoid allowed cold winter air temperatures to penetrate the subsurface and the permafrost body to cool the shallow subsurface so that soil temperatures were below 0°C. Hence, snowmelt could readily infiltrate below the shrubs, while the frozen conditions of the graminoid prevented infiltration of liquid water. This is confirmed by the shallow soil moisture sensors. In the shrubs, a clear increase in liquid water content was recorded, while the value in the graminoid remained unchanged until the graminoid became snow free and shallow temperatures started to increase. Within the shrubs, liquid water content at 0.4m bgl remained constant throughout the snowmelt event, indicating fully saturated conditions. Hence, changes in the deeper parts of the imaging transect indicate processes similar to the rainfall event, in that snowmelt is providing energy to the deeper permafrost system, causing changes to the permafrost temperature and unfrozen water content.

Once the graminoid became snow free and warm air temperatures led to thawing of the surficial layer, snowmelt started to infiltrate. Heterogeneities within the graminoid, microtopography, and presence of near surface permafrost (x = 65m) caused variable changes in the upper 5m bgl. Areas known to be characterized by near surface permafrost and microtopographic highs showed small changes in the shallow subsurface (x = 65m and 75m, respectively), while depressions showed more pronounced changes. Interestingly, the deeper subsurface (>5m bgl) showed a continuous decrease in resistivity. Investigating the spatio-temporal changes in the graminoid area (Fig. 3D-F) showed that lateral flow from the shrub areas caused decreasing resistivities below the graminoid. Hence, lateral flow is expected to be a significant factor in the formation and development of taliks at this site.

Changes occurred most rapidly underneath the western shrubs. Four weeks after the snowmelt event the trend reverses and resistivities are increasing slightly (Fig. 3E), particularly in the shallow subsurface. This shows that the snowmelt pulse traveled through the system quickly, and indicates that thermal and hydraulic conductivities are likely higher below the western than the eastern shrubs, where changes occurred at slower rates and remained longer.

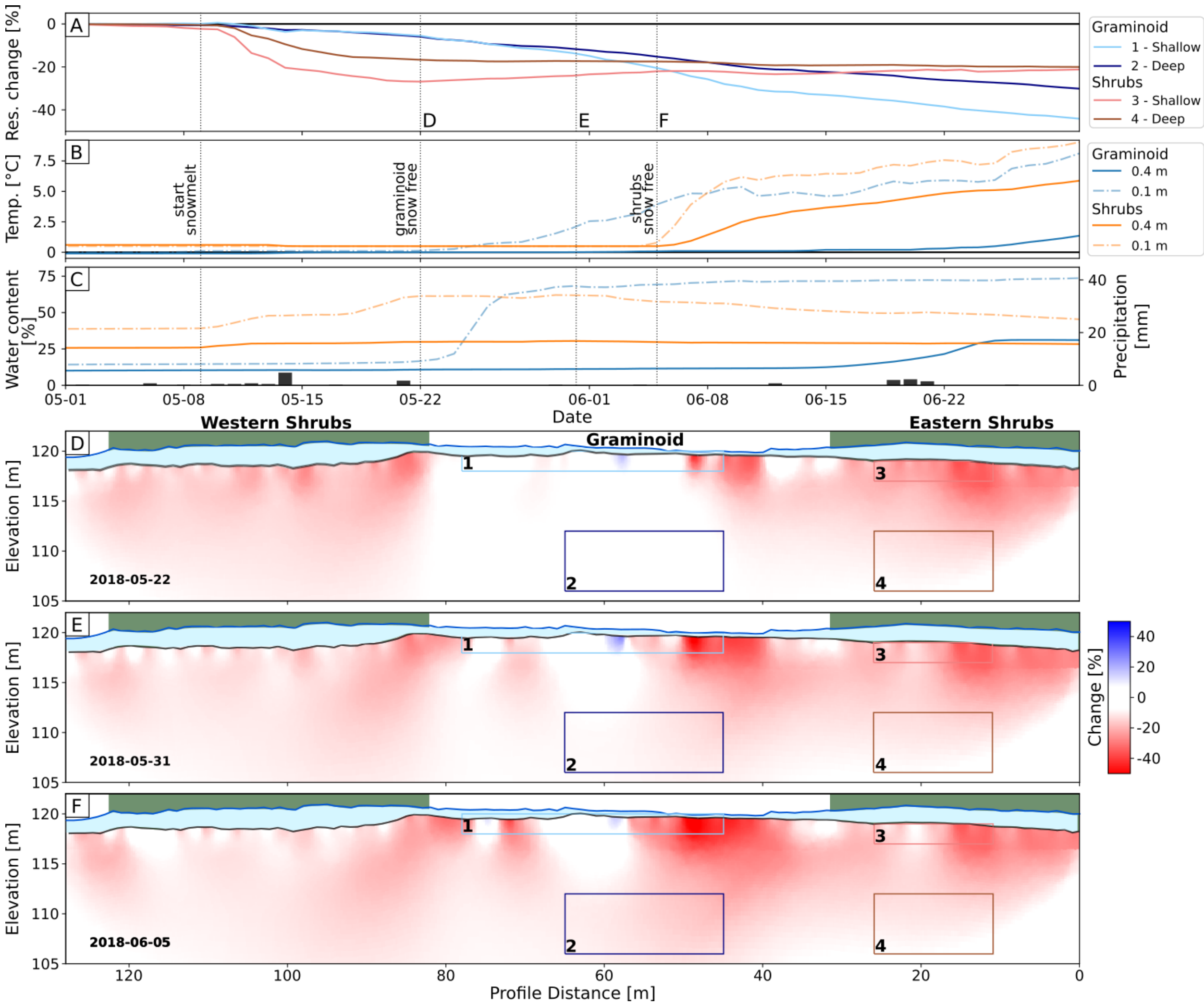

Figure 3 Snowmelt is causing rapid change in electrical resistivity, particularly underneath the shrubs. (A) Change in electrical resistivity relative to measurements prior to the start of snowmelt (05/01/2018). (B-C) variation in soil temperature and moisture content, and precipitation. (D-F) distribution of changes in electrical resistivity at three dates past snowmelt event. Indicated snow thickness corresponds to measurements in 04/2018.

6 Inter-annual thermohydrological dynamics

Although rainfall and snowmelt events provide insights about permafrost thermohydrological processes, investigation of longer-term dynamics is needed to explore the evolution of permafrost systems. Fig. 4 shows the resistivity distribution at the beginning of the monitoring period in September 2017, and changes in resistivity with respect to that measurement for the end of August 2018, and from 2018 to 2019 (Fig. 4B and C, respectively). These measurements are representative of the warmest subsurface temperatures, reached at the end of summer. Changes in resistivity from 2017 to 2018 (Fig. 4B) are different in the shallow and deep subsurface. The shallow subsurface (<3m bgl) is characterized by increasing resistivity, which can be related to a decreasing trend in soil moisture, and hence drier conditions. From 2018 to 2019 (Fig. 4C) this trend reverses and decreasing resistivities were recorded. This is in agreement with a wetter summer of 2019 compared to 2018. The deeper subsurface shows a decreasing trend over the two years, with the strongest changes being observed in the area underneath the graminoid.

To quantify these effects, we performed a laboratory analysis of the temperature-electrical relationship of soil samples obtained along the monitoring transect (for details see supplementary information). Fig. 4D shows data from two samples, sandy and silty loams, which present the two end members of recovered samples in terms of their electrical behavior, as well as the bilinear temperature-resistivity relationships for those samples. At temperatures above 0°C, increasing temperatures decrease resistivity by about 2%/°C, while between -2 and -0.5°C resistivity decreases by about 67%/°C due to decreasing ice content.

Employing these relationships, we converted the time series of electrical resistivity of deep (between 8 and 14 m bgl) permafrost units into temperature (Fig. 4E-F). Due to the uncertainty in the subsurface properties' variations, the range in estimated temperatures is large. The results show an annual variability with minimum temperatures in late spring, and maximum temperatures in late summer. For the graminoid area (Fig. 4E), September 2017 were on average -0.76°C, while below the eastern and western shrubs temperatures were slightly warmer at -0.72°C and -0.66°C (Fig. 4F), respectively. Temperature was on average 0.20°C higher at the end of summer 2019 than recorded in 2017 (0.11°C higher in 2018). Given the uncertainties in the subsurface properties and related petrophysical relationships, temperatures during this two-year period increased by at least 0.09°C. During the same period, a temperature sensor at 1.5m bgl recorded an increase of 0.08°C, at a location where a smaller resistivity change was observed (-16.9% compared to -37.9%). Starting at slightly warmer temperatures, eastern and western shrubs had deep temperatures increasing by about 0.12 and 0.11°C, respectively. Here, direct temperature measurements at 1.5m depth showed consistently unfrozen conditions, and end of summer temperatures increased by 2.22 and 2.05°C in the eastern and western shrubs, respectively. This change in unfrozen conditions would relate to an about 4% change in resistivity, and hence is in agreement with the 3.8% observed change.

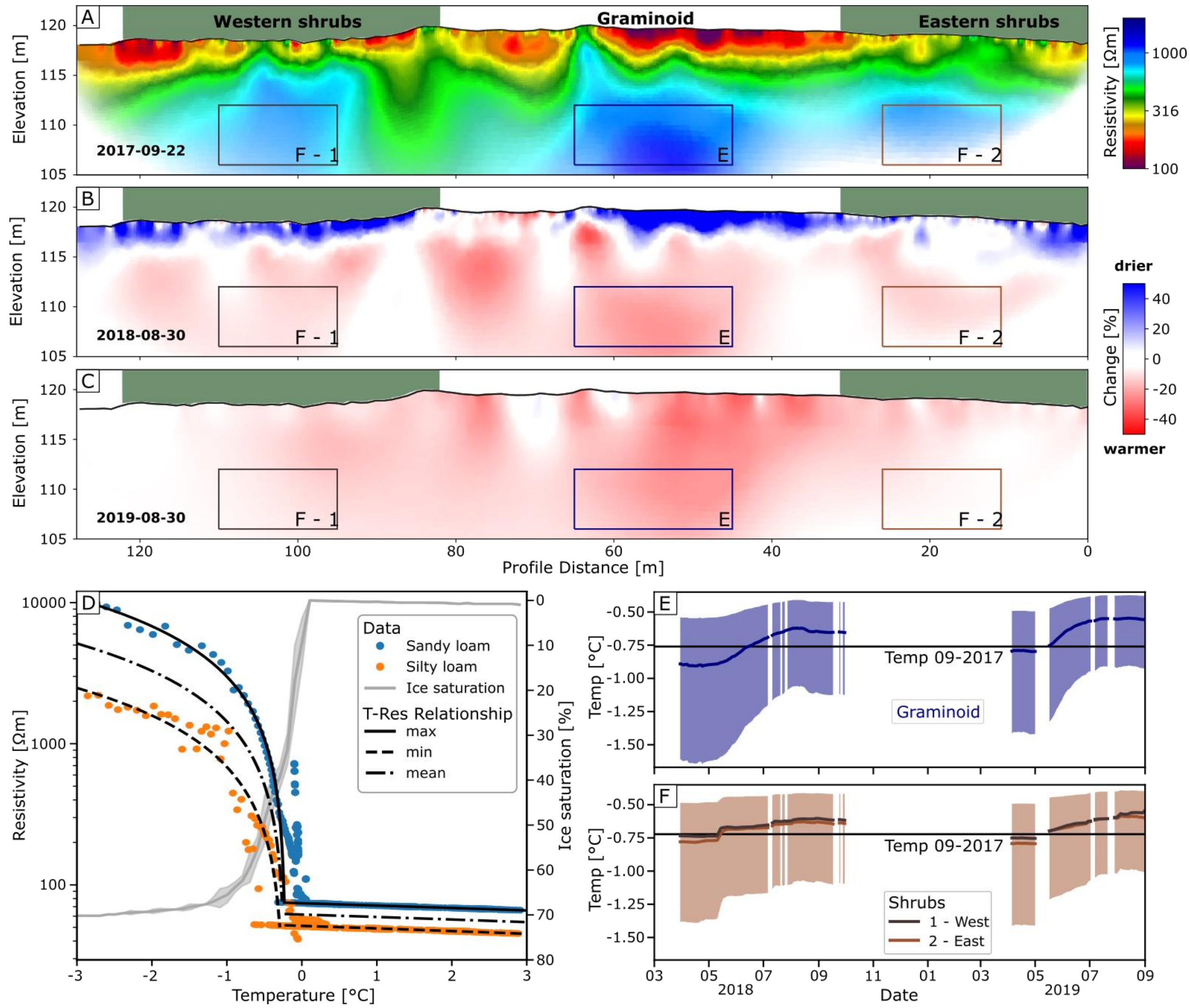

Figure 4 Electrical resistivity indicating variable subsurface warming of up to 0.2°C within a two year period. (A) Baseline resistivity model indicating areas analyzed in (E) and (F). Distribution of annual changes in resistivity from the start of monitoring in September 2017 to the end of summer of (B) 2018, and (C) from 2018 to 2019. (D) Laboratory-derived temperature-resistivity relationship. (E-F) temperature variation for deep permafrost bodies (boxes in A-C) derived from applying the petrophysical relationship.

7 Discussion and Conclusion

We investigated the subsurface response to both rapid and longer term perturbations along a transect located in a transitional, discontinuous permafrost environment on the Seward Peninsula. Our analysis highlights that the thermohydrological response to snowmelt and rainfall in this transitional permafrost environment is rapid and penetrates to depths of >10m. The data show that the response of these systems is driven by the heterogeneity in snowpack, which at this scale is highly influenced by vegetation and topography. Rapid propagation of snowmelt and precipitation energy were observed in shrub dominated landscapes, while the frozen ground below the thin snowpack of graminoid areas prevented rapid and deep movement. While observed on a local scale, we expect those processes to be representative for similar environments throughout the Arctic.

Our results show a clear increasing trend in permafrost temperatures over the two year monitoring period. Larger changes were recorded in the graminoid, which showed higher resistivities and hence lower temperatures at the start of the monitoring period. Assuming similar climatic conditions, the estimated temperatures and temperature changes would likely cause permafrost at this site to disappear within the next decade. These conclusions are robust to common uncertainties associated with geoelectrical measurements (see supporting information for more detail). Given the expected increase in winter snow accumulation and increased frequency of summer atmospheric rivers, these processes may even be accelerated, as the thicker snow pack will better insulate the ground from freezing temperatures, and early summer rainfall will easily infiltrate into the subsurface, thereby driving advective heat transport into the permafrost bodies. Projecting local observations to regional trends, the southern Seward Peninsula may see a transition from a discontinuous permafrost environment to sporadic occurrences of permafrost within the next few decades, which is supported by recent modelling studies (Debolskiy et al., 2020). This will impact hydrological fluxes, where increasing hydraulic conductivities will enable improved infiltration through and drainage of shallow soil layers, resulting in a change to plant water availability throughout the year. This will also result in significant changes to latent and sensible heat fluxes (Yoshikawa & Hinzman, 2003), and likely alter greenhouse gas emissions, resulting in increasing CO_2 and decreasing CH_4 emissions (Lawrence et al., 2015). These changes will be accompanied by changes in vegetation types, as has been seen in response to wildfires and rapidly degrading permafrost in other areas (Frost et al., 2020). Although this study focused on a natural ecosystem, even faster changes can be expected for developed areas, with severe impacts on infrastructure and communities due to permafrost thaw.

Acknowledgments

We acknowledge the assistance of Berkeley Lab's Geoscience Measurement Facility for enabling the ERT monitoring system. This research has been supported by the Office of Biological and Environmental Research in the DOE Office of Science (grant no. DE-AC02-05CH11231). Data of this study is available from the NGEE Arctic data portal (https://doi.org/10.5440/1728709).

References

Biskaborn, B. K., Smith, S. L., Noetzli, J., Matthes, H., Vieira, G., Streletskiy, D. A., et al. (2019). Permafrost is warming at a global scale. *Nature Communications*, *10*(1), 264. https://doi.org/10.1038/s41467-018-08240-4

Bring, A., Fedorova, I., Dibike, Y., Hinzman, L., Mård, J., Mernild, S. H., et al. (2016). Arctic terrestrial hydrology: A synthesis of processes, regional effects, and research challenges. *Journal of Geophysical Research: Biogeosciences*, *121*(3), 621–649. https://doi.org/10.1002/2015JG003131

Brown, J., Ferrians, O., Heginbottom, J. A., & Melnikov, E. (2002). *Circum-Arctic Map of Permafrost and Ground-Ice Conditions, Version 2*. Boulder, Colorado USA.

Busey, B., Bolton, B., Wilson, C., & Cohen, L. (2017). Surface Meteorology at Teller Site Stations, Seward Peninsula, Alaska, Ongoing from 2016. https://doi.org/10.5440/1437633

Chen, L., Fortier, D., McKenzie, J. M., & Sliger, M. (2020). Impact of heat advection on the thermal regime of roads built on permafrost. *Hydrological Processes*, *34*(7), 1647–1664. https://doi.org/10.1002/hyp.13688

Dafflon, B., Oktem, R., Peterson, J., Ulrich, C., Tran, A. P., Romanovsky, V., & Hubbard, S. S. (2017). Coincident aboveground and belowground autonomous monitoring to quantify covariability in permafrost, soil, and vegetation properties in Arctic tundra. *Journal of Geophysical Research: Biogeosciences*, *122*(6), 1321–1342. https://doi.org/10.1002/2016JG003724

Debolskiy, M. V., Nicolsky, D. J., Hock, R., & Romanovsky, V. E. (2020). Modeling Present and Future Permafrost Distribution at the Seward Peninsula, Alaska. *Journal of Geophysical Research: Earth Surface*, *125*(8), 1–24. https://doi.org/10.1029/2019JF005355

Farzamian, M., Vieira, G., Monteiro Santos, F. A., Yaghoobi Tabar, B., Hauck, C., Catarina Paz, M., et al. (2020). Detailed detection of active layer freeze-thaw dynamics using quasi-continuous electrical resistivity tomography (Deception Island, Antarctica). *Cryosphere*, *14*(3), 1105–1120. https://doi.org/10.5194/tc-14-1105-2020

Frost, G. V., Loehman, R. A., Saperstein, L. B., Macander, M. J., Nelson, P. R., Paradis, D. P., & Natali, S. M. (2020). Multi-decadal patterns of vegetation succession after tundra fire on the Yukon-Kuskokwim Delta, Alaska. *Environmental Research Letters*, *15*(2), 025003. https://doi.org/10.1088/1748-9326/ab5f49

Hinzman, L. D., Kane, D. L., Gieck, R. E., & Everett, K. R. (1991). Hydrologic and thermal properties of the active layer in the Alaskan Arctic. *Cold Regions Science and Technology*, *19*(2), 95–110. https://doi.org/10.1016/0165-232X(91)90001-W

Hinzman, L. D., Bettez, N. D., Bolton, W. R., Chapin, F. S., Dyurgerov, M. B., Fastie, C. L., et al. (2005). Evidence and implications of recent climate change in Northern Alaska and other Arctic regions. *Climatic Change*, *72*(3), 251–298. https://doi.org/10.1007/s10584-005-5352-2

Hjort, J., Karjalainen, O., Aalto, J., Westermann, S., Romanovsky, V. E., Nelson, F. E., et al. (2018). Degrading permafrost puts Arctic infrastructure at risk by mid-century. *Nature Communications*, *9*(1). https://doi.org/10.1038/s41467-018-07557-4

Ireson, A. M., van der Kamp, G., Ferguson, G., Nachshon, U., & Wheater, H. S. (2013). Hydrogeological processes in seasonally frozen northern latitudes: understanding, gaps and challenges. *Hydrogeology Journal*, *21*(1), 53–66. https://doi.org/10.1007/s10040-012-0916-5

Jansson, J. K., & Taş, N. (2014). The microbial ecology of permafrost. *Nature Reviews Microbiology*, *12*(6), 414–425. https://doi.org/10.1038/nrmicro3262

Johnson, T. C., Versteeg, R. J., Ward, A., Day-Lewis, F. D., & Revil, A. (2010). Improved hydrogeophysical characterization and monitoring through parallel modeling and inversion of time-domain resistivity and induced-polarization data. *Geophysics*, *75*(4), WA27. https://doi.org/10.1190/1.3475513

Jorgenson, M. T., Romanovsky, V., Harden, J., Shur, Y., O'Donnell, J., Schuur, E. A. G., et al. (2010). Resilience and vulnerability of permafrost to climate change. *Canadian Journal of Forest Research*, *40*(7), 1219–1236. https://doi.org/10.1139/X10-060

Jorgenson, M. T., Harden, J., Kanevskiy, M., O'Donnell, J., Wickland, K., Ewing, S., et al. (2013). Reorganization of vegetation, hydrology and soil carbon after permafrost degradation across heterogeneous boreal landscapes. *Environmental Research Letters*, *8*(3), 035017. https://doi.org/10.1088/1748-9326/8/3/035017

Kneisel, C., Hauck, C., Fortier, R., & Moorman, B. (2008). Advances in geophysical methods for permafrost investigations. *Permafrost and Periglacial Processes*, *19*(2), 157–178.

Koch, J. C., Runkel, R. L., Striegl, R., & McKnight, D. M. (2013). Hydrologic controls on the transport and cycling of carbon and nitrogen in a boreal catchment underlain by continuous permafrost. *Journal of Geophysical Research: Biogeosciences*, *118*(2), 698–712. https://doi.org/10.1002/jgrg.20058

Krautblatter, M., Verleysdonk, S., Flores-Orozco, A., & Kemna, A. (2010). Temperature-calibrated imaging of seasonal changes in permafrost rock walls by quantitative electrical resistivity tomography (Zugspitze, German/Austrian Alps). *Journal of Geophysical Research*, *115*(F2), 1–15.

Lawrence, D. M., Koven, C. D., Swenson, S. C., Riley, W. J., & Slater, A. G. (2015). Permafrost thaw and resulting soil moisture changes regulate projected high-latitude CO2 and CH4 emissions. *Environmental Research Letters*, *10*(9). https://doi.org/10.1088/1748-9326/10/9/094011

Léger, E., Dafflon, B., Robert, Y., Ulrich, C., Peterson, J. E., Biraud, S. C., et al. (2019). A distributed temperature profiling method for assessing spatial variability in ground temperatures in a discontinuous permafrost region of Alaska. *Cryosphere*, *13*(11), 2853–2867. https://doi.org/10.5194/tc-13-2853-2019

Lloyd, A. H., Yoshikawa, K., Fastie, C. L., Hinzman, L., & Fraver, M. (2003). Effects of permafrost degradation on woody vegetation at arctic treeline on the Seward Peninsula, Alaska. *Permafrost and Periglacial Processes*, *14*(2), 93–101. https://doi.org/10.1002/ppp.446

Lyon, S. W., Mörth, M., Humborg, C., Giesler, R., & Destouni, G. (2010). The relationship between subsurface hydrology and dissolved carbon fluxes for a sub-arctic catchment. *Hydrology and Earth System Sciences*, *14*(6), 941–950. https://doi.org/10.5194/hess-14-941-2010

Mekonnen, Z. A., Riley, W. J., Grant, R. F., & Romanovsky, V. (2020). Changes in precipitation and air temperature contribute comparably to permafrost degradation in a warmer climate. *Environmental Research Letters*, *in press*.

Ming, F., Li, D. Q., & Chen, L. (2020). Electrical Resistivity of Freezing Clay: Experimental Study and Theoretical Model. *Journal of Geophysical Research: Earth Surface*, *125*(2), 1–18. https://doi.org/10.1029/2019JF005267

Minsley, B. J., Abraham, J. D., Smith, B. D., Cannia, J. C., Voss, C. I., Jorgenson, M. T., et al. (2012). Airborne electromagnetic imaging of discontinuous permafrost. *Geophysical Research Letters*, *39*(2), 1–8. https://doi.org/10.1029/2011GL050079

Neumann, R. B., Moorberg, C. J., Lundquist, J. D., Turner, J. C., Waldrop, M. P., McFarland, J. W., et al. (2019). Warming Effects of Spring Rainfall Increase Methane Emissions From Thawing Permafrost. *Geophysical Research Letters*, *46*(3), 1393–1401. https://doi.org/10.1029/2018GL081274

Oldenburg, D. W., & Li, Y. (1999). Estimating depth of investigation in dc resistivity and IP surveys. *Geophysics*, *64*(2), 403–416. https://doi.org/10.1190/1.1444545

Parsekian, A. D., Creighton, A. L., Jones, B. M., & Arp, C. D. (2019). Surface nuclear magnetic resonance observations of permafrost thaw below floating, bedfast, and transitional ice lakes. *GEOPHYSICS*, *84*(3), EN33–EN45. https://doi.org/10.1190/geo2018-0563.1

Petrone, K. C., Jones, J. B., Hinzman, L. D., & Boone, R. D. (2006). Seasonal export of carbon, nitrogen, and major solutes from Alaskan catchments with discontinuous permafrost. *Journal of Geophysical Research: Biogeosciences*, *111*(G2), n/a-n/a. https://doi.org/10.1029/2005JG000055

Rowland, J. C., Travis, B. J., & Wilson, C. J. (2011). The role of advective heat transport in talik development beneath lakes and ponds in discontinuous permafrost. *Geophysical Research Letters*, *38*(17), n/a-n/a. https://doi.org/10.1029/2011GL048497

Thomas, H. R., Cleall, P., Li, Y.-C., Harris, C., & Kern-Luetschg, M. (2009). Modelling of cryogenic processes in permafrost and seasonally frozen soils. *Géotechnique*, *59*(3), 173–184. https://doi.org/10.1680/geot.2009.59.3.173

Tso, C. M., Kuras, O., Wilkinson, P. B., Uhlemann, S., Chambers, J. E., Meldrum, P. I., et al. (2017). Improved characterisation and modelling of measurement errors in electrical resistivity tomography (ERT) surveys. *Journal of Applied Geophysics*, *146*, 103–119. https://doi.org/10.1016/j.jappgeo.2017.09.009

Vincent, W. F., Lemay, M., & Allard, M. (2017). Arctic permafrost landscapes in transition: towards an integrated Earth system approach. *Arctic Science*, *3*(2), 39–64. https://doi.org/10.1139/as-2016-0027

Walvoord, M. A., & Kurylyk, B. L. (2016). Hydrologic Impacts of Thawing Permafrost-A Review. *Vadose Zone Journal*, *15*(6), vzj2016.01.0010. https://doi.org/10.2136/vzj2016.01.0010

Woo, M.-K., Kane, D. L., Carey, S. K., & Yang, D. (2008). Progress in permafrost hydrology in the new millennium. *Permafrost and Periglacial Processes*, *19*(2), 237–254. https://doi.org/10.1002/ppp.613

Wu, Y., Nakagawa, S., Kneafsey, T. J., Dafflon, B., & Hubbard, S. (2017). Electrical and seismic response of saline permafrost soil during freeze - Thaw transition. *Journal of Applied Geophysics*, *146*, 16–26. https://doi.org/10.1016/j.jappgeo.2017.08.008

Yoshikawa, K., & Hinzman, L. D. (2003). Shrinking thermokarst ponds and groundwater dynamics in discontinuous permafrost near council, Alaska. *Permafrost and Periglacial Processes*, *14*(2), 151–160. https://doi.org/10.1002/ppp.451

Zhang, T., Barry, R., Knowles, K., Ling, F., & Armstrong, R. (2003). Distribution of seasonally and perennially frozen ground in the Northern Hemisphere. In *Proceedings of the 8th International Conference on Permafrost* (pp. 1289–1294). Zürich, Switzerland: AA Balkema Publishers. https://doi.org/10.1007/978-3-642-61317-3_3